Dalton Transactions

ROYAL SOCIETY OF CHEMISTRY

PAPER

View Article Online
View Journal | View Issue

Cite this: *Dalton Trans.*, 2022, **51**, 13061

Diaryl dithiocarbamates: synthesis, oxidation to thiuram disulfides, Co(III) complexes $[Co(S_2CNAr_2)_3]$ and their use as single source precursors to CoS_2†

Jagodish C. Sarker, [a,b] Rosie Nash,[a] Suwimon Boonrungsiman,[c] David Pugh [a] and Graeme Hogarth *[a]

Received 6th June 2022,
Accepted 6th August 2022

DOI: 10.1039/d2dt01767a

rsc.li/dalton

Air and moisture stable diaryl dithiocarbamate salts, Ar_2NCS_2Li, result from addition of CS_2 to Ar_2NLi, the latter being formed upon deprotonation of diarylamines by ^{n}BuLi. Oxidation with $K_3[Fe(CN)_6]$ affords the analogous thiuram disulfides, $(Ar_2NCS_2)_2$, two examples of which (Ar = *p*-C_6H_4X; X = Me, OMe) have been crystallographically characterised. The interconversion of dithiocarbamate and thiuram disulfides has also been probed electrochemically and compared with that established for the widely-utilised diethyl system. While oxidation reactions are generally clean and high yielding, for Ph(2-naphthyl)NCS_2Li an *ortho*-cyclisation product, 3-phenylnaphtho[2,1-*d*]thiazole-2(3*H*)-thione, is also formed, resulting from a competitive intramolecular free-radical cyclisation. To demonstrate the coordinating ability of diaryl dithiocarbamates, a small series of Co(III) complexes have been prepared, with two examples, $[Co\{S_2CN(p\text{-tolyl})_2\}_3]$ and $[Co\{S_2CNPh(m\text{-tolyl})\}_3]$ being crystallographically characterised. Solvothermal decomposition of $[Co\{S_2CN(p\text{-tolyl})_2\}_3]$ in oleylamine generates phase pure CoS_2 nanospheres in an unexpected phase-selective manner.

Introduction

Dithiocarbamates (DTCs) are versatile ligands that find widespread use in coordination chemistry, due (in part) to their ease of synthesis and also the synthesis of their complexes.[1] For dialkyl-DTCs, synthesis is usually as simple as dissolving a secondary amine in water (or alcohol) in the presence of base (NaOH and KOH are most widely used), followed by (slow) addition of CS_2 and stirring at room temperature for a short time.[1–3] This procedure, which is also applicable to aryl–alkylamines,[4] requires no special equipment, conditions or chemicals, thus allowing access to these ligands in laboratories worldwide. A common misconception regarding their preparation is that the corresponding amide is initially generated,[5] which subsequently undergoes nucleophilic attack at CS_2. This is incorrect, and it is easy to show that the bases generally used (NaOH, KOH, NEt_3, *etc.*) are not basic enough to deprotonate secondary amines. Rather, reactions proceed *via* direct attack of the amine on CS_2 resulting in formation of a zwitterionic intermediate,[6] which is deprotonated to afford the desired salt (Scheme 1a), and the reaction kinetics have been shown to be very sensitive to the nature of the amine.[7,8]

Diarylamines are significantly less basic than their dialkyl or alkyl–aryl counterparts, as seen from a comparison of aqueous pK_a values for Et_2NH (10.98), PhEtNH (4.17) and Ph_2NH (0.79). Consequently, and despite a number of reports to the contrary,[9–12] diaryl-DTCs cannot be prepared upon addition of the amine to CS_2 in the presence of alkali metal hydroxides or tertiary amines. The synthesis of NaS_2CNPh_2 has been reported upon addition of excess NaH to Ph_2NH followed by CS_2 addition,[13–15] and also from the (slow) reaction (*ca.* 24 h) of Ph_2NH with $NaNH_2$ (again followed by CS_2 addition) in benzene,[16,17] but in our hands the NaH route has proved difficult to reproduce. In 1995, Snaith and co-workers reported a high yielding synthesis of LiS_2CNPh_2 from the reaction of Ph_2NLi with CS_2 in toluene, the amide being generated upon deprotonation of Ph_2NH by ^{n}BuLi at −70 °C (Scheme 1b).[18] While this synthesis must be carried out under an inert atmosphere, the high yields and simple work-up procedure were appealing to us, and others have also identified the utility of this route.[19,20]

A current focus is the use of DTC complexes as single source precursors (SSPs) towards nanoscale metal-

[a]*Department of Chemistry, King's College London, Britannia House, 7 Trinity Street, London SE1 1DB, UK. E-mail: graeme.hogarth@kcl.ac.uk*
[b]*Department of Chemistry, Jagannath University, Dhaka-1100, Bangladesh*
[c]*Centre for Ultrastructural Engineering, King's College London, New Hunt's House, London SE1 1UL, UK*

†Electronic supplementary information (ESI) available. CCDC 2175344–2175348. For ESI and crystallographic data in CIF or other electronic format see DOI: https://doi.org/10.1039/d2dt01767a

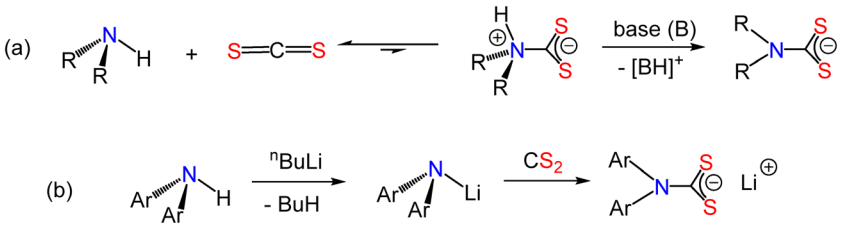

Scheme 1 Synthetic routes to (a) dialkyl (and alkyl–aryl) and (b) diaryl DTC salts.

sulfides.[21–26] We, and others, have focused almost exclusively on the use of dialkyl-DTC derivatives,[27] and as far as we are aware there are no substantiated reports of the use of diaryl-DTC complexes as SSPs. Herein we describe the synthesis and characterisation of a small series of diaryl-DTC salts, together with initial studies on the formation of thiuram disulfides (TDS), themselves useful precursors to metal–DTC complexes.[28] We also report the synthesis of octahedral d^6-cobalt (III) complexes, which serve as exemplars for this type of ligand coordination, and their use as SSPs, decomposing in oleylamine to afford CoS_2 nanomaterials.

Results and discussion

Synthesis of dithiocarbamate salts Ar_2NCS_2Li

We followed the method of Snaith and co-workers,[18,29] also adopted by Wei,[29] for the synthesis of LiS_2CNPh_2 (**1a**) to prepare a range of diaryl-DTC salts (**1a–g**) (Scheme 2). The diarylamine was dissolved in THF and cooled to −78 °C. Upon addition of ^{n}BuLi the solution turned pale yellow, being associated with formation of the corresponding amide, Ar_2NLi, but no attempts were made to isolate these. To ensure complete reaction, the solution was slowly (*ca.* 1 h) warmed to room temperature. For CS_2 addition it was cooled back to 0 °C using an ice bath and CS_2 added dropwise resulting in formation of a thick orange precipitate. After warming to room temperature, volatiles were removed on a rotary evaporator and the resulting solid redissolved in a minimum amount of warm toluene to give a clear orange solution. Cooling this solution led to the reprecipitation of a microcrystalline orange solid which was collected by filtration and dried. Yields are high, sometimes *ca.* 100%, which we associate with water coordination at lithium even after redispersal in toluene. Once dry, they can be stored at room temperature in air and as far as we can measure there is no discernible decomposition over prolonged periods (*ca.* 3 years) at room temperature.

All show a low field signal at *ca.* 219 ppm in the $^{13}C\{^1H\}$ NMR spectrum, being associated with the quaternary backbone carbon of the DTC, the position of which varies little upon changing substituents. This can be compared with that for NaS_2CNEt_2 at *ca.* 207.5 ppm.[30] Other signals in both the ^1H NMR and $^{13}C\{^1H\}$ NMR spectra are similar to those in the parent amines. IR spectra of dialkyl-DTCs contain peaks associated with ν(C–N) in the range of 1450–1580 cm^{-1} and between 940–1060 cm^{-1} associated with the asymmetric ν(C–S).[1,30] For **1a**, these absorptions are seen at 1490 and 1045 cm^{-1} respectively. Electrospray ionisation mass spectrometry (ESI-MS) data for **1** do not show a molecular ion, but base peaks are consistent with $Ar_2NCS_2^+$ fragments (*i.e.* M^+ – Li).

We did not attempt to characterise **1** by X-ray diffraction but note that in Snaith's original paper he reports the structure of **1a** recrystallised from THF.[18] This shows the coordination of two molecules of THF and confirms the chelate nature of the DTC, with lithium adopting a distorted tetrahedral geometry. The C–N bond of 1.364(3) Å shows some degree of double bond character and can be compared to that of *ca.* 1.33–1.36 Å in dialkyl DTCs and 1.41–1.44 Å in pyrrole and pyrrolidine DTCs.[31] Importantly the two phenyl rings are orientated approximately perpendicular to the LiS_2CN plane (*ca.* 80–87°) suggesting that there is no conjugation of the aryl groups with the DTC functionality. Thus, while these substituents can still be considered as electron-withdrawing, as noted from the $^{13}C\{^1H\}$ NMR chemical shift, they are not fully conjugated. This view is also supported by the UV-vis spectrum of **1b** which shows two strong absorptions at 263 and 293 cm^{-1} for **1b** being associated with π–π* transitions characteristic of the NCS_2 moiety,[31] being comparable with those of simple dialkyl-DTC salts. In contrast, carbazole-DTCs, in which the aromatic ring is constrained to lie in the same plane as the NCS_2 unit, also show a third band at *ca.* 340–350 nm attributed to intramolecular charge transfer from the NCS_2 group to the aromatic ring, a feature missing from the UV-vis spectrum of **1**.

While the route for preparation of diaryl DTCs using ^{n}BuLi is convenient and high yielding, the use of a pyrophoric base under inert conditions means that it cannot be used in less well-equipped laboratory environments. A number of groups

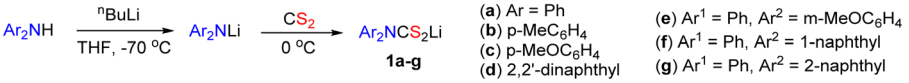

Scheme 2 Synthesis of lithium DTC salts **1a–g**.

have previously reported the formation of KS_2CNPh_2 from reaction of Ph_2NH and CS_2 in the presence of KOH,[32–34] but as was the case for NaOH, in our hands this reaction did not work. Tatsumi and co-workers reported that $KNPh_2$ can be prepared from $HNPh_2$ and KO^{t}Bu in THF[35] and taking inspiration from this, we stirred a solution of $(p\text{-tolyl})_2NH$, KO^{t}Bu and CS_2 in THF for 24 h at room temperature, which gave a yellow suspension affording $KS_2CN(p\text{-tolyl})_2$ (**1h**), small pale-yellow crystals in 70% yields after workup. Characterising data are similar to that of the lithium salt **2b**, the quaternary carbon appearing at 218.3 ppm. Thus, while we have not developed the KO^{t}Bu route is seems accessible and applicable in a non-specialist laboratory setting. We also note that the phosphonium salt $[PPh_4][S_2CNPh_2]$[36] has been reported, being prepared upon mixing stoichiometric amounts of $[Ph_4P]Br$ and NaS_2CNPh_2 in MeCN, but $^{13}C\{^1H\}$ NMR data were not given.

Synthesis of thiuram disulfides $(Ar_2NCS_2)_2$

Dailkyl-DTCs are readily oxidised to the corresponding thiuram disulfides (TDS), one of which, Et_4TDS (disulfiram), is an FDA-approved alcohol-aversive agent for the treatment of alcohol dependence,[37] while both disulfiram and other TDSs have been shown to have a variety of other biological functions.[38–41] Compared to tetra-alkylthiuram disulfides (R_4TDS), the corresponding tetra-aryl derivatives, Ar_4TDS, are relatively unstudied,[41] although they do have applications in pseudo-living free radical polymerization[42,43] and have been tested as inhibitors of lymphoid tyrosine phosphatase.[44]

We chose $K_3[Fe(CN)_6]$ as the oxidising agent since it is self-indicating (Scheme 3).[45] Dropwise addition of an aqueous solution of $K_3[Fe(CN)_6]$ (*ca.* 0.6 M) to **1a–g** suspended in water resulted in formation of off-white precipitates. These were taken up in CH_2Cl_2, separated from the water, and dried to afford **2a–g** in *ca.* 50–80% yields. We suspect that reactions proceed in high (*ca.* quantitative) yields but isolating the product is not always simple. Thus, solids are quite "claggy" and not easily separated by filtration, while their solubility in CH_2Cl_2 varies depending upon the substituents. Once isolated, they are dry off-white solids that can be stored indefinitely in air. In the $^{13}C\{^1H\}$ NMR spectrum, the quaternary backbone carbon is now seen at *ca.* 197 ppm and ^1H NMR spectra are somewhat broader than those for the diaryl-DTC salts, presumably resulting from restricted rotation about the S–S bond.

Unlike other diaryl-DTCs, the 2-naphthyl-*N*-phenyl derivative **1g** oxidised to give a mixture of the expected Ar_4TDS **2g**, along with a red *ortho*-cyclisation product, 3-phenylnaphtho[2,1-*d*]thiazole-2(3*H*)-thione, $C_{17}H_{11}NS_2$ (**2h**) (Scheme 4). Thus, after crystallisation a mixture of crystals of **2g** and **2h** resulted which were separated manually. While **2h** has been described in the literature, being prepared in 74% yield upon refluxing 3-phenyl-6,7-benzobenzothiazolone and P_2S_5 in xylene, no characterising data was presented.[46] Benzothiazolethiones show interesting biological properties and are normally prepared from the corresponding 1-iodo, 2-amino arenes.[47,48] Elemental analysis, IR and ^1H and $^{13}C\{^1H\}$ NMR data are consistent with the molecular formula, but very similar to those for **2g** except the heterocyclic thioketo group, –S–C═S signal in the $^{13}C\{^1H\}$ NMR spectrum which appears at δ 197.5, while the thioureide signal in **2h** is at δ 189.5. A plausible mechanism of co-formation of **2g** and **2h** is shown (Scheme 4). Presumably, the close proximity of the *ortho*-naphthyl proton to the sulfur centre allows a competitive intra-molecular radical addition reaction alongside the expected radical dimerization.

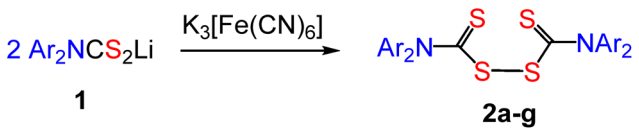

Scheme 3 Synthesis of tetra-arylthiuram disulfides (**2a–g**).

Synthesis of cobalt complexes $[Co(S_2CNAr_2)_3]$

Diamagnetic Co(III) d^6 complexes have a distorted octahedral coordination environment and are easily prepared.[1] In beginning to probe the coordinating ability of diaryl-DTCs we felt that such complexes would be a good starting point as other

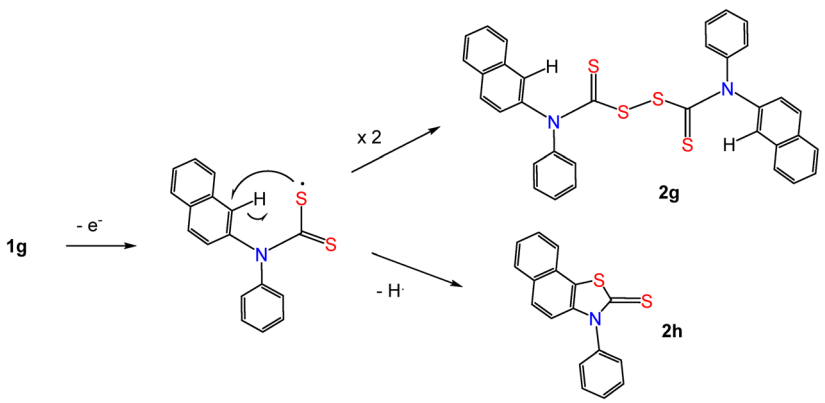

Scheme 4 Proposed mechanism of co-formation of **2g** and **2h**.

M(III) octahedral complexes such as Fe(III) and Mn(III) are paramagnetic[1] and thus difficult to characterise using NMR spectroscopy. The synthesis of $[Co(S_2CNPh_2)_3]$ (**3a**) was first reported (but no characterising data given) in 1979[49] using NaS_2CNPh_2 as the DTC source, the latter being formed by the method of Kupchik and Calabretta, using sodium amide as a base.[16]

In a similar manner to the reactions with dialkyl-DTC salts, addition of cobalt(II) acetate to *ca.* three equivalents of **1a–g** in water resulted in immediate formation of a green precipitate and simple work up afforded high yields (*ca.* 90%) of green $[Co(S_2CNAr_2)_3]$ (**3a–g**) (Scheme 5). Due to the quadrupolar effect of cobalt, NMR signals are broad, and the quaternary carbon signal was not visible in $^{13}C\{^1H\}$ NMR spectra, while signals in ^1H NMR spectra did not show J_{HH} couplings. Each gave a molecular ion peak in the EIMS and elemental analyses and IR spectra are fully consistent with proposed formulations.

Molecular structures

We have elucidated the molecular structures of $[(p\text{-}MeC_6H_4)_2NCS_2]_2$ (**2b**), $[(p\text{-}MeOC_6H_4)_2NCS_2]_2$ (**2c**), $C_{17}H_{11}NS_2$ (**2h**), $[Co\{S_2CN(p\text{-tolyl})_2\}_3]$ (**3b**) and $[Co\{S_2CNPh(m\text{-tolyl})\}_3]$ (**3e**) by X-ray crystallography (Fig. 1–3). A summary of the crystallographic data and refinement parameters is given in Table S1† and selected bond lengths and angles are given in the ESI.†

Molecular structures of a number of dialkyl[50–55] and alkyl–aryl TDS[56,57] have previously been reported and gross structural features of diaryl derivatives are similar. The structure of **2c** is crystallographically straightforward (Fig. 1b) its centrosymmetric nature and C–S–S–C torsional angle of 180° being previously observed for $^iPr_4TDS$.[53] In contrast, that of **2b** is more complicated as there is a whole-molecule disorder (Fig. 1a). Thus, there are two orientations in a *ca.* 84 : 16 ratio (major form is shown) differing with respect to the C–S–S–C torsional angle [97.7(1) and −104.3(1)°]. These can be compared with the C–S–S–C torsion angles of 85.8° (R = ^{i}Bu),[52] 96.4° (R = Et)[50] and 89.27° (R = CH_2CH_2OMe).[52] A second important metric parameter is the S–S bond distance which is normally *ca.* 2.0 Å. Distances of 2.0139(4) and 2.0861(6) Å in **2b** and **2c** respectively are slightly longer than those found in the dialkyl derivatives, while in the ethyl-phenyl derivative it is similar at 2.0112(5) Å.[57]

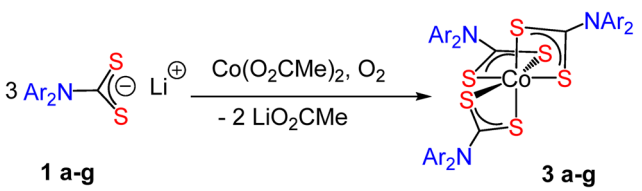

Scheme 5 Synthesis of $[Co(S_2CNAr_2)_3]$ (**3a–g**).

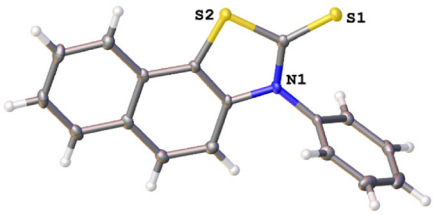

Fig. 2 Molecular structure of one (of six) independent molecules of **2h** showing 50% probability thermal ellipsoids.

The molecular structure of one independent molecule of **2h** is shown in Fig. 2. Crystallographically it is unusual as there are six independent molecules in the asymmetric unit but fortunately (and somewhat remarkably) there is no disorder. The major difference between the six is the dihedral angle between the plane of the phenyl ring and the plane defined by the 13 atoms of the activated naphthyl group.

Many Co(III) DTCs have been characterised crystallographically[57–64] and in all the metal adopts a distorted octahedral coordination environment with average Co–S bond lengths of *ca.* 2.26 Å. White and co-workers[60] showed that the effects of different alkyl substituents on the structures of $[Co(S_2CNR_2)_3]$ is minor. This is also true for bis(*p*-tolyl) (**3b**) and Ph(*m*-anisyl) (**3e**) analogues (Fig. 3). [For **3e** each molecule contains a disordered *m*-anisyl group.] Average S–Co–S bite angle and *trans* S–Co–S angles are 77.06 (2), 164.46(2) **3b**; and 76.53

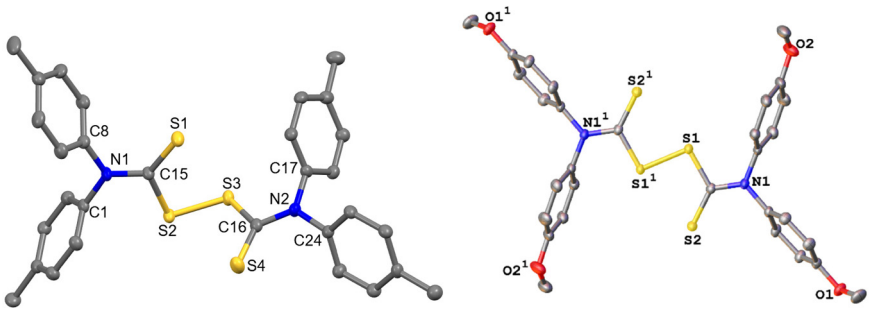

Fig. 1 Molecular structures of (a) one conformer of **2b** and (b) **2c** showing 50% probability thermal ellipsoids with hydrogen atoms omitted for clarity.

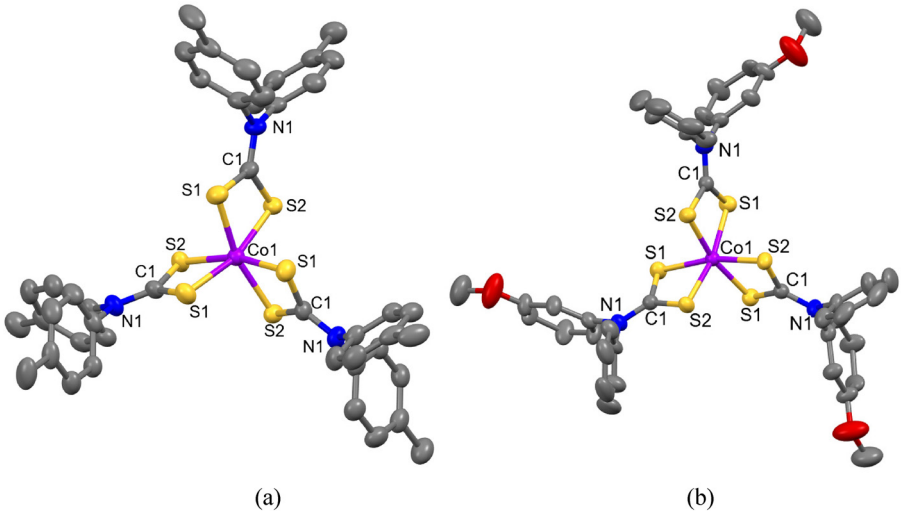

Fig. 3 Molecular structures of (a) $[Co\{S_2CN(p\text{-tolyl})_2\}_3]$ (**3b**) and (b) $[Co\{S_2CNPh(m\text{-anisyl})_2\}_3]$ (**3e**).

(2), 166.82(2) **3e** being very similar to those in dialkyl-derivatives. Dihedral angles do change significantly when aryl groups are introduced. Thus, dihedral angle between alkyl/aryl groups are *ca.* 1.3°,[63] 17.1 for EtH,[58] *ca.* 74 for EtPh,[57] *ca.* 77° for **3b** and *ca.* 70° for **3e**.

Electrochemistry

DTCs are chemically oxidized to the corresponding TDS, a process that can be addressed electrochemically (Scheme 6). The DTC first undergoes a quasi-reversible oxidation, which is followed by a coupling reaction to form the corresponding TDS, thus oxidation of $Et_2NCS_2^-$ occurs at 0.09 V *vs.* Ag/AgCl (*ca.* −0.4 V *vs.* Cp_2Fe^+/Cp_2Fe) corresponding to formation of Et_4TDS.[65,66] This coupling step is chemically reversible, forming an equilibrium that heavily favours the TDS, the cleavage of which is kinetically slow,[68,69] and the position of this equilibrium is sensitive to the nature of the substituents.[70] Similarly, cleavage of TDS may also be achieved electrochemically[68,69] for which two pathways are viable. In the gas phase, reduction followed by S–S bond cleavage is energetically preferred, but in solution a concerted bond-breaking electron-transfer mechanism is predicted to be equally probable. Lieder has studied standard potentials of the DTC–TDS redox system *via* thermochemical cycles and computational electrochemistry.[67]

Fig. 4 displays experimental electrochemical data for **1b**–**2b** and maintain the key characteristics of the dialkyl redox behaviour. At 0.5 V s^{-1} (in MeCN), reduction of **2b** occurs at $E_{peak(a)}$ = −2.02 V (*vs.* $Fc^{+/0}$); a 260 mV cathodic shift as compared to that seen for Et_4TDS (Fig. S1†). Scanning back in the positive direction leads to the expected oxidation of the $[DTC]^-$ that is generated at the electrode upon cleavage of $[TDS]^-$. For **1b** this oxidation occurs at $E_{peak(c)}$ = −0.298 V, as compared to $E_{peak(c)}$ = −0.348 V for $[Et_2DTC]^-$. The peak separation for **2b** is 1.722 V, being around 210 mV smaller than the 1.932 V peak separation observed for Et_4TDS under these conditions. At slower scan rates (<0.1 V s^{-1}), back oxidation of **2b** is not observed, which suggests an instability of the **1b** at the electrode surface. This is in contrast to Et_4TDS where back-oxidation is seen at <0.05 V s^{-1}. At suitably high scan rates (>2.0 V s^{-1}) a broad plateau is observed *ca.* −1.4 V, a feature also present (but not as distinct) for slower scan rates, as well as for Et_4TDS. This may result from reduction of the DTC radical, which could be stabilised by the delocalised electron character of the aryl groups, which is very similar to the proposed model as well as the experimental results for $^iPr_4TDS$.[71,72]

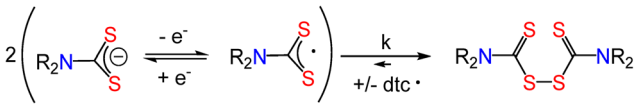

Scheme 6 Redox interchange between DTCs and TDS.

$[Co(S_2CNAr_2)_3]$ as single source precursors (SSPs) to CoS_2

As detailed in the introduction, DTC complexes find widespread use as SSPs towards a range of nanoscale metal-sulfides[27] and a major driver for our development of the chemistry of diaryl-DTC complexes as SSPs. A range of cobalt sulfides are known including CoS_2 (cattierite) which has the pyrite structure and Co_3S_4 (linnaeite) which adopts the spinel motif, while CoS, Co_2S_3 and Co_9S_8 are also known, the latter being the cobalt analogue of pentlandite. A target for many researchers is CoS_2 as it is intrinsically a conductive metal and excellent electrocatalyst.[73–75]

Nomura and Nakai first reported the use of a cobalt DTC complex as SSPs in 2003, showing that chemical vapour deposition (CVD) of $[Co(S_2CNEt_2)_3]$ at 450 °C gave thin films of cubic Co_9S_8.[76] Soon after, O'Brien and co-workers reported the deposition of a phase pure Co_3S_4 film from $[Co(S_2CNMeHex)_3]$ at 450 °C.[77] Solvothermal decomposition of cobalt DTCs has not been widely studied. Thirumaran and co-workers decomposed furfuryl complexes $[Co(S_2CNR_2)_3]$ and $[Co(S_2CNRBz)_3]$ (R = $CH_2C_4H_3O$) in triethylenetetramine to give nanorods of Co_3S_4,[78] while Revaprasadu and co-workers have reported that

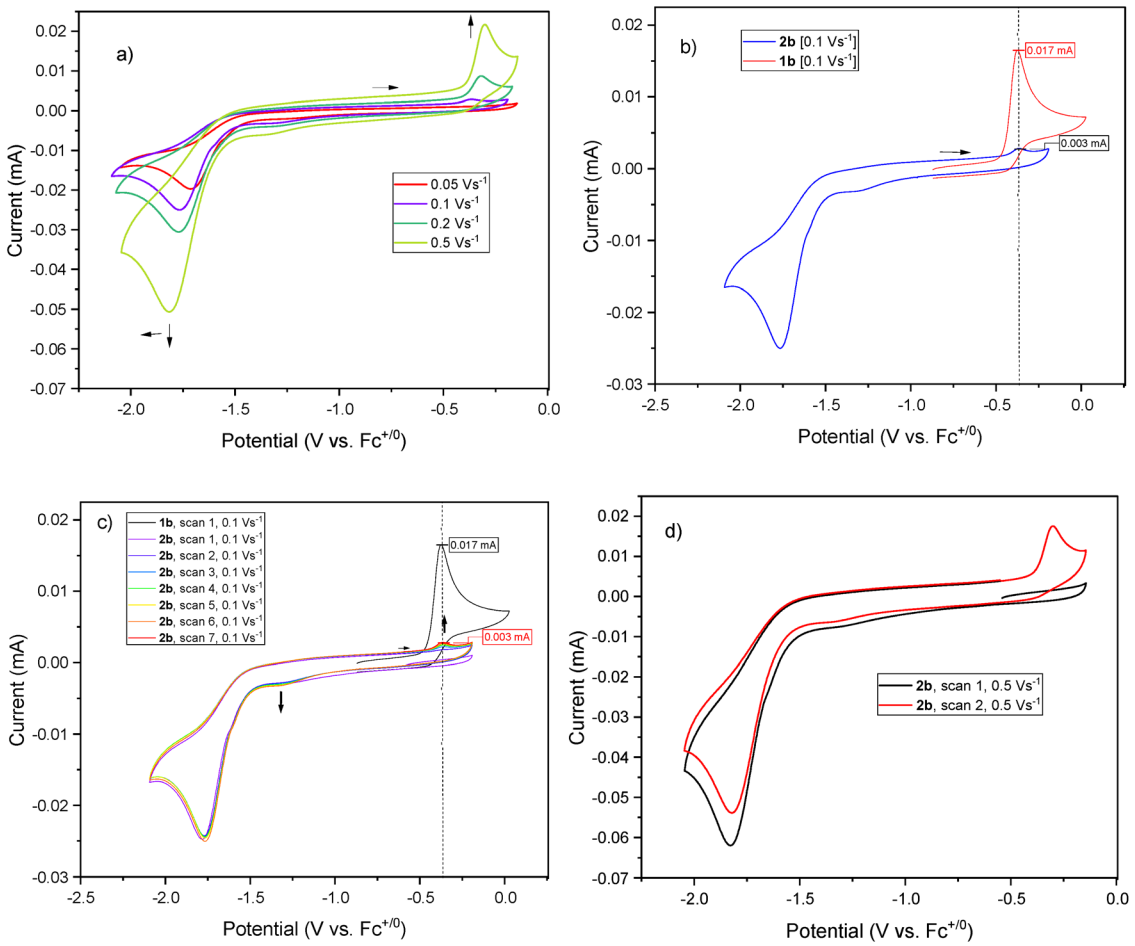

Fig. 4 CVs for **2b** at 0.05, 0.1, 0.2, 0.5 V s^{-1} (a), **2b** *vs.* **1b** at 0.1 V s^{-1} (b), increase of the oxidation peak current over time/scan at 0.1 V s^{-1} (c) and increase of the oxidation peak current over time/scan at 0.5 V s^{-1} (d) of 1 mM solution in MeCN with 100 mM of $[NBu_4][PF_6]$ as supporting electrolyte. Data collected on a 3 mm diameter glassy carbon working electrode, with a platinum counter electrode and a silver wire reference electrode.

hot injection (HI) of $[Co(S_2CNC_8H_8O)_3]$ in oleylamine (OLA) affords nanoplates of CoS.[79] There are also reports of Co(II) complexes $[Co(S_2CNR_2)_2]$[80–84] being used as SSPs, although as these are extremely oxygen sensitive, they are most likely to be the Co(III) complexes.[1] Most notably, ultra-thin, defect-rich, Co_9S_8 nanosheets have been prepared by Li and co-workers from decomposition of (putative) $[Co(S_2CNBu_2)_2]$ at 220 °C in oleic acid in the presence of excess PPh_3.[85] Importantly, as far as we are aware, cobalt DTC SSPs have not previously been used to generate CoS_2.

To this end we have carried out preliminary studies on the solvothermal decomposition of **3b** in oleylamine (OLA) using heat up (HU) and hot-injection (HI) methods. At room temperature **3b** is partially soluble in OLA and as the temperature is increased it slowly dissolves to give an ever-darker green solution which is clear (indicative of stability) up to *ca.* 180 °C. Above this temperature, the solution turns black and becomes darker as the temperature is raised to *ca.* 230 °C being maintained there for 1 h. After slowly cooling to room temperature,

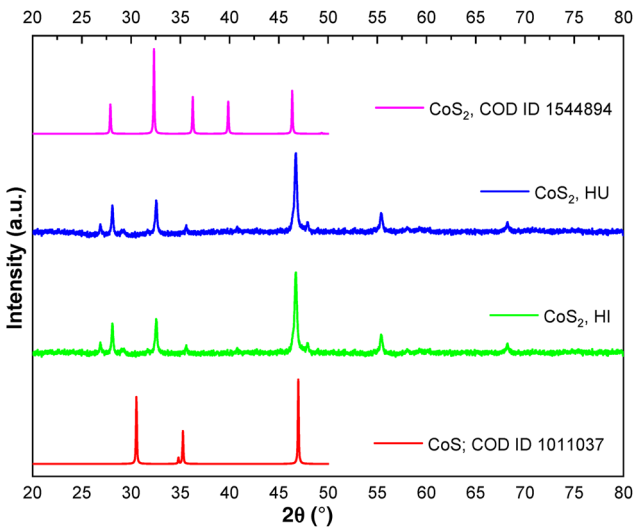

Fig. 5 PXRD of CoS_2 produced from **3b** by HI and HU.

MeOH was added to precipitate the generated black nanoparticles, which were isolated by standard procedures (see Experimental section). For HI process, OLA (15 mL) was heated to 230 °C for 15 min and **3b** (300 mg in 5 mL OLA at 80 °C) injected into the flask. Immediately, the colour changed from green to black and the solution was maintained at 230 °C for 1 h followed by standard workup.

Powder XRD (Fig. 5) of both samples from HU and HI revealed the crystalline phase of the decomposed black powders to be CoS_2 (cattierite). The peak at 46.7°2θ for the (220) lattice plane is more intense than in the reference pattern, suggesting preferred growth in this direction. A small peak at *ca.* 26° is unaccounted for. TEM images (Fig. 6) for particles generated by the HI method show that they are predominantly nanospheres with an average diameter of 580 nm. Unfortunately, we have been unable to record suitable TEM images of the HU sample to date.

The important finding here is that solvothermal decomposition in OLA of **3b** cleanly affords CoS_2 nanospheres. An aim of our work is to understand the molecules to materials process and in previous work on di-iso-butyl DTCs of Ni (II),[24,25] Zn(II)[21] and Fe(III)[23] we have utilised *in situ* EXAFS studies and DFT calculations to probe decomposition mechanism(s). Unfortunately we have not yet been able to do this for Co(III) complexes, but can reflect on findings for the closely related d^5 complex $[Fe(S_2CN^iBu_2)_3]$.[23] This shows three distinct decomposition steps; (i) amine coordination with formation of monodentate DTC ligands (up to 60 °C), (ii) reductive-elimination of DTC to afford Fe(II) species above 90 °C, (iii) amine-exchange to generate $[Fe(S_2CNHR)(S_2CNR_2)]$ and/or $[Fe(S_2CNHR)_2]$ which rapidly decompose to iron sulfides. For $[Co(S_2CNAr_2)_3]$ a major difference is the high crystal field stabilisation energy (CFSE) resulting from the low spin d^6 configuration, while $[Fe(S_2CNR_2)_3]$ and $[Fe(S_2CNAr_2)_3]$ are spin crossover complexes, and likely the high spin (CFSE = 0) form is that which decomposes.[23] The high CFSE of **3b** is seen in the maintenance of its structural integrity up to *ca.* 180 °C, as evidenced by the lack of colour change or any turbidity noted in the HU process. Thus, decomposition probably occurs catastrophically above 180 °C, which is supported by the similar product formation from HU and HI methods. With the accessibility of Co(II) bis(dithiocarbamate) complexes, it is tempting to suggest that reductive-elimination of TDS is the first step in this process (following from that established for iron), being followed by the fast amine-exchange to give afford $[Co(S_2CNHR)_2]$ (R = oleyl) which in turn rapidly eliminates two equivalents of RNCS to leave CoS_2. Thus, we have previously established that while amine-exchange is fast at four-coordinate centres, it is much slower at six-coordinate centres, something we have rationalised in terms of an intramolecular process requiring metal pre-coordination of the primary amine (Scheme 7).[27]

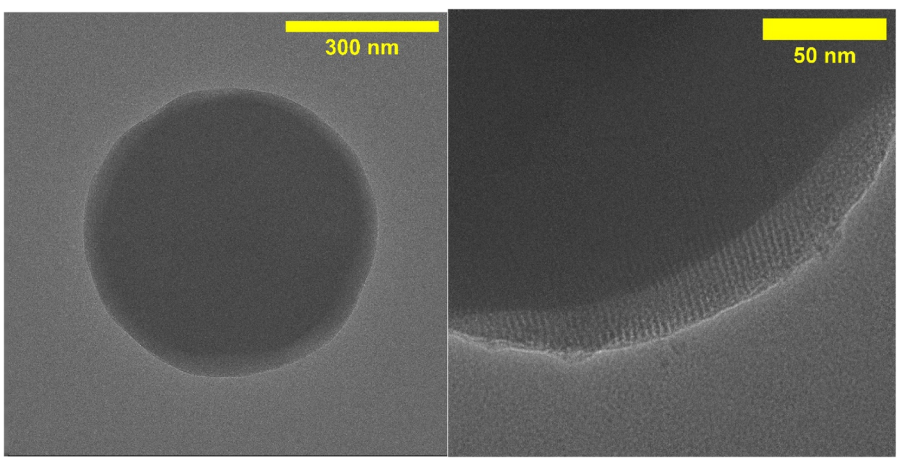

Fig. 6 TEM image of CoS_2 nanosphere produced from **3b** by HI.

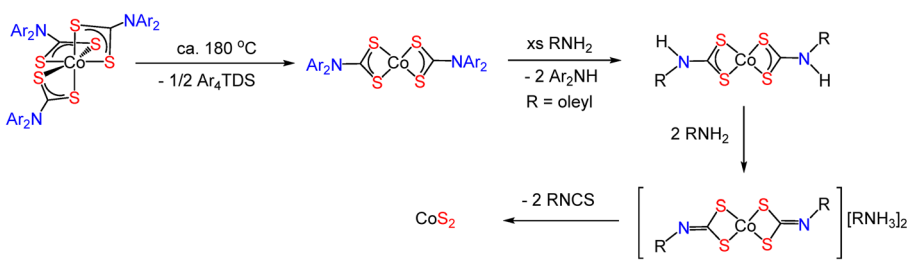

Scheme 7 Plausible scheme for the formation of CoS_2 from $[Co(S_2CNAr_2)_3]$ in OLA (RNH_2).

Exclusive formation of CoS_2 upon decomposition of **3b** in OLA contrasts with the report of Revaprasadu and co-workers who heated $[Co(S_2CNC_8H_8O)_3]$ in the same solvent to form hexagonal CoS at both 200 and 260 °C.[79] They did, however, note that the quality of their PXRD data was poor and thus there is some uncertainty over this assignment. Interestingly, when the same SSP was studied by TGA the residue mass was consistent with formation of CoS_2. Clearly further work is required here but the preliminary data suggest that Co(III) diaryl-DTC complexes may be a fruitful source of CoS_2 and we are currently carrying out further decomposition experiments on **3a–g** while also targeting aniline-derived complexes $[Co(S_2CNHAr)_3]$ which have briefly been mentioned in the literature[85] but have not been considered as SSPs.

Summary and conclusions

While DTCs have been widely studied over the past century most activity has focussed on dialkyl derivatives and, in comparison, diaryl-DTCs have been largely neglected. Here we begin to rebalance this and show that a range of lithium salts, LiS_2CNAr_2, are easily prepared upon addition of CS_2 to Ar_2NLi, themselves being formed upon deprotonation of the amines by ^{n}BuLi at −78 °C. Diaryldithiocarbamate salts are air and moisture stable and can be easily stored for long periods, and for labs that do not have access to facilities to use pyrophoric organometallic reagents, we show that the potassium salt $KS_2CN(p\text{-tolyl})_2$ can be prepared using the easy-to-handle $KOBu^t$ as a base. Similar to dialkyl analogues, diaryl-DTC salts are oxidised by $K_3[Fe(CN)_6]$ to produce the respective thiuram disulfides, Ar_4TDS, a reversible process that we have probed by cyclic voltammetry. To show the utility of diaryl-DTCs as ligands, we have prepared a small series of Co(III) complexes, two of which have been crystallographically characterised. Structurally they are very similar to the dialkyl-analogues, and we note that the aryl groups are rotated out of the CoS_2N plane, thus not being conjugated with this DTC ring system. This is also supported by UV-vis spectra of the lithium salts which show two strong absorption bands (at 263 and 293 cm^{-1} for **1b**) but no band above 350 cm^{-1} associated with a conjugated π-system.[31] Preliminary solvothermal decomposition of $[Co\{S_2CN(tolyl)_2\}_3]$ (**3b**) by both HI and HU methods leads to clean formation of phase pure cattierite (CoS_2) nanospheres, which have applications in electrocatalysis.[73–75] This appears to be the first time DTC SSPs have been used to prepare CoS_2 and this suggests a potentially important utility of $[Co(S_2CNAr_2)_3]$ and (we speculate) $[Co(S_2CNHAr)_3]$ for the preparation of this technologically important material.

Conflicts of interest

There are no conflicts to declare.

Acknowledgements

We thank the Commonwealth Scholarship commission for a PhD studentship to JCS (grant no. BDCS-2018-52) and King's College London for a PhD studentship to RN. SB thanks the European Commission for the award of a Marie Curie Fellowship (grant no. 893404).

References

1 G. Hogarth, *Prog. Inorg. Chem.*, 2005, **53**, 71–561.
2 F. Jian, Z. Wang, Z. Bai, X. You, H.-K. Fun, K. Chinnakali and I. A. Razak, *Polyhedron*, 1999, **18**, 3401–3406.
3 H. Yin, F. Li and D. Wang, *J. Coord. Chem.*, 2007, **60**, 1133–1141.
4 P. A. Ajibade, D. C. Onwudiwe and M. J. Moloto, *Polyhedron*, 2011, **30**, 246–252.
5 D. C. Onwudiwe and P. A. Ajibade, *Int. J. Mol. Sci.*, 2011, **12**, 1964–1978.
6 W.-D. Rudorf, *J. Sulfur Chem.*, 2007, **28**, 295–339.
7 E. A. Castro, R. Cortés, J. G. Santos and J. C. Vega, *J. Org. Chem.*, 1982, **47**, 3774–3777.
8 E. A. Castro, S. A. Pena, J. G. Santos and J. C. Vega, *J. Org. Chem.*, 1984, **49**, 863–866.
9 A. M. Paca and P. A. Ajibade, *Mater. Chem. Phys.*, 2017, **202**, 143–150.
10 K. S. Siddiqi, S. A. A. Nami, Lutfullah and Y. Chebude, *Synth. React. Inorg., Met.-Org., Nano-Met. Chem.*, 2005, **35**, 445–451.
11 S. Singhal, A. N. Garg and K. Chandra, *Transition Met. Chem.*, 2005, **30**, 44–52.
12 S. Khan, W. Ahmad, K. S. Munawar and S. Kanwal, *Indian J. Pharm. Sci.*, 2018, **80**, 480–488.
13 P. Vella and J. Zubieta, *J. Inorg. Nucl. Chem.*, 1978, **40**, 477–487.
14 M. Uchiyama, K. Satoh and M. Kamigaito, *Angew. Chem., Int. Ed.*, 2015, **54**, 1924–1928.
15 K. G. Molloy, *Inorg. Chem.*, 1988, **27**, 677–681.
16 E. J. Kupchik and P. J. Calabretta, *Inorg. Chem.*, 1965, **4**, 973–978.
17 H. Ma, G. Wang, G. T. Yee, J. L. Petersen and M. P. Jensen, *Inorg. Chim. Acta*, 2009, **362**, 4563–4569.
18 S. C. Ball, I. Cragg-Hine, M. G. Davidson, R. P. Davies, A. J. Edwards, I. Lopez-Solera, P. R. Raithby and R. Snaith, *Angew. Chem., Int. Ed. Engl.*, 1995, **34**, 921–923.
19 J. A. Baus and R. Tacke, *Dalton Trans.*, 2017, **46**, 8751–8755.
20 G.-Z. Lu, N. Su, H.-Q. Yang, Q. Zhu, W.-W. Zhang, Y.-X. Zheng, L. Zhou, J.-L. Zuo, Z.-X. Chen and H.-J. Zhang, *Chem. Sci.*, 2019, **10**, 3535–3542.
21 H.-U. Islam, A. Roffey, N. Hollingsworth, W. Bras, G. Sankar, N. H. De Leeuw and G. Hogarth, *Nanoscale Adv.*, 2020, **2**, 798–807.
22 A. Roffey, N. Hollingsworth and G. Hogarth, *Nanoscale Adv.*, 2019, **1**, 3056–3066.

23 G. Hogarth, N. Hollingsworth, H. Islam, W. Bras, N. H. De Leeuw, A. Roffey and G. Sankar, *Nanoscale Adv.*, 2019, **1**, 2965–2978.
24 A. Roffey, N. Hollingsworth, H.-U. Islam, M. Mercy, G. Sankar, C. R. A. Catlow, G. Hogarth and N. H. de Leeuw, *Nanoscale*, 2016, **8**, 11067–11075.
25 N. Hollingsworth, A. Roffey, H.-U. Islam, M. Mercy, A. Roldan, W. Bras, M. Wolthers, C. R. A. Catlow, G. Sankar, G. Hogarth and N. H. de Leeuw, *Chem. Mater.*, 2014, **26**, 6281–6292.
26 P. B. Mann, I. J. McGregor, S. Bourke, M. Burkitt-Gray, S. Fairclough, M. T. Ma, G. Hogarth, M. Thanou, N. Long and M. Green, *Nanoscale Adv.*, 2019, **1**, 522–526.
27 J. C. Sarker and G. Hogarth, *Chem. Rev.*, 2021, **121**, 6057–6123.
28 L. I. Victoriano, *Coord. Chem. Rev.*, 2000, **196**, 383–398.
29 P. Padungros and A. Wei, *Synth. Commun.*, 2014, **44**, 2336–2343.
30 H. L. M. Van Gaal, J. W. Diesveld, F. W. Pijpers and J. G. M. Van der Linden, *Inorg. Chem.*, 1979, **18**, 3251–3260.
31 A. W. De Martino, M. L. Souza and P. C. Ford, *Chem. Sci.*, 2017, **8**, 7186–7196.
32 D. Zhang, J. Chen, Y. Liang and H. Zhou, *Synth. Commun.*, 2005, **35**, 521–526.
33 A. K. Mishra and N. K. Kaushik, *Spectrochim. Acta, Part A*, 2008, **69**, 842–848.
34 M. Shahnaz, Namrata, J. Sharma, J. Parkash and D. N. Parsad, *J. Drug Delivery Ther.*, 2013, **3**, 110–114.
35 J. Ito, Y. Ohki, M. Iwata and K. Tatsumi, *Inorg. Chem.*, 2008, **47**, 3763–3771.
36 C. M. Donahue, I. K. Black, S. L. Pecnik, T. R. Savage, B. L. Scott and S. R. Daly, *Polyhedron*, 2014, **75**, 110–117.
37 B. Cvek, *Curr. Cancer Drug Targets*, 2011, **11**, 332–337.
38 Z. Skrott, M. Mistrik, K. K. Andersen, S. Friis, D. Majera, J. Gursky, T. Ozdian, J. Bartkova, Z. Turi, P. Moudry, M. Kraus, M. Michalova, J. Vaclavkova, P. Dzubak, I. Vrobel, P. Pouckova, J. Sedlacek, A. Miklovicova, A. Kutt, J. Li, J. Mattova, C. Driessen, Q. P. Dou, J. Olsen, M. Hajduch, B. Cvek, R. J. Deshaies and J. Bartek, *Nature*, 2017, **552**, 194–199.
39 Q. Spillier, D. Vertommen, S. Ravez, R. Marteau, Q. Themans, C. Corbet, O. Feron, J. Wouters and R. Frederick, *Sci. Rep.*, 2019, **9**, 1–9.
40 C. N. Kapanda, G. G. Muccioli, G. Labar, J. H. Poupaert and D. M. Lambert, *J. Med. Chem.*, 2009, **52**, 7310–7314.
41 J. C. Jochims, *Chem. Ber.*, 1968, **101**, 1746–1752.
42 K. Jiang, S. Han, M. Ma, L. Zhang, Y. Zhao and M. Chen, *J. Am. Chem. Soc.*, 2020, **142**, 7108–7115.
43 G. Moad, *J. Polym. Sci., Part A: Polym. Chem.*, 2019, **57**, 216–227.
44 R. A. Kulkarni, S. M. Stanford, N. A. Vellore, D. Krishnamurthy, M. R. Bliss, R. Baron, N. Bottini and A. M. Barrios, *ChemMedChem*, 2013, **8**, 1561–1568.
45 P. J. Nichols and M. W. Grant, *Aust. J. Chem.*, 1989, **42**, 1085–1101.
46 I. K. Ushenko, *Sb. Statei Obshch. Khim.*, 1953, **1**, 516–522.
47 N. Srivastava and R. Kishore, *J. Sulfur Chem.*, 2021, **42**, 29–39.
48 X. Zhu, W. Li, X. Luo, G. Deng, Y. Liang and J. Liu, *Green Chem.*, 2018, **20**, 1970–1974.
49 L. R. Gahan, J. G. Hughes, M. J. O'Connor and P. J. Oliver, *Inorg. Chem.*, 1979, **18**, 933–937.
50 I. L. Karle, J. A. Estlin and K. Britts, *Acta Crystallogr.*, 1967, **22**, 273–280.
51 G. A. Williams, J. R. Statham and A. H. White, *Aust. J. Chem.*, 1983, **36**, 1371–1377.
52 P. R. Fontenot, B. Wang, Y. Chen and J. P. Donahue, *Acta Crystallogr., Sect. E: Crystallogr. Commun.*, 2017, **73**, 1764–1769.
53 V. Kumar, G. Aravamudan and M. Seshasayee, *Acta Crystallogr., Sect. C: Cryst. Struct. Commun.*, 1990, **C46**, 674–676.
54 G. C. Rout, M. Seshasayee and G. Aravamudan, *Cryst. Struct. Commun.*, 1982, **11**, 1389–1393.
55 M. M. Karim, M. N. Abser, M. R. Hassan, N. Ghosh, H. G. Alt, I. Richards and G. Hogarth, *Polyhedron*, 2012, **42**, 84–88.
56 I. Raya, I. Baba, F. Z. Rosli and B. M. Yamin, *Acta Crystallogr., Sect. E: Struct. Rep. Online*, 2005, **E61**, o3131–o3132.
57 P. A. Ajibade, B. C. Ejelonu and B. Omondi, *Acta Crystallogr., Sect. E: Struct. Rep. Online*, 2012, **E68**, 02182.
58 G.-L. Zhang, Y.-T. Li and Z.-Y. Wu, *Acta Crystallogr., Sect. E: Struct. Rep. Online*, 2006, **E62**, m350–m351.
59 J. Granell, M. L. H. Green, V. J. Lowe, S. R. Marder, P. Mountford, G. C. Saunders and N. M. Walker, *J. Chem. Soc., Dalton Trans.*, 1990, 605–614.
60 P. C. Healy, J. W. Connor, B. W. Skelton and A. H. White, *Aust. J. Chem.*, 1990, **43**, 1083–1095.
61 P. C. Healy, J. V. Hanna, N. V. Duffy and B. W. Skelton, *Aust. J. Chem.*, 1990, **43**, 1335–1346.
62 F. F. Jian, F. L. Beia, P. S. Zhao, X. Wang, H. K. Fun and K. Chinnakali, *J. Coord. Chem.*, 2002, **55**, 429–437.
63 H. Iwasaki and K. Kobayashi, *Acta Crystallogr., Sect. B: Struct. Crystallogr. Cryst. Chem.*, 1980, **36**, 1657–1659.
64 T. C. Woon, M. F. Mackay and M. J. O'Connor, *Inorg. Chim. Acta*, 1982, **58**, 5–11.
65 A. M. Bond, R. Colton, A. F. Hollenkamp, B. F. Hoskins and K. McGregor, *J. Am. Chem. Soc.*, 1987, **109**, 1969–1980.
66 G. Cauquis and D. Lachenal, *J. Electroanal. Chem.*, 1973, **43**, 205–213.
67 M. Lieder, *Phosphorus, Sulfur Silicon Relat. Elem.*, 2003, **178**, 179–189.
68 S. J. Visco, C. C. Mailhe, L. C. De Jonghe and M. B. Armand, *J. Electrochem. Soc.*, 1989, **136**, 661–664.
69 M. Liu, S. J. Visco and L. C. De Jonghe, *J. Electrochem. Soc.*, 1989, **136**, 2570–2575.
70 M. Liu, S. J. Visco and L. C. De Jonghe, *J. Electrochem. Soc.*, 1990, **137**, 750–759.
71 E. Potteau, L. Nicolle, E. Levillain and J.-P. Lelieur, *Electrochem. Commun.*, 1999, **1**, 360–364.

72 P. J. Nichols and M. W. Grant, *Aust. J. Chem.*, 1982, **35**, 2455–2463.
73 C. Scrimager and L. J. Dehayes, *Inorg. Nucl. Chem. Lett.*, 1978, **14**, 125–133.
74 M. S. Faber, M. A. Lukowski, Q. Ding, N. S. Kaiser and S. Jin, *J. Phys. Chem. C*, 2014, **118**, 21347–21356.
75 M. S. Faber, K. Park, M. Caban-Acevedo, P. K. Santra and S. Jin, *J. Phys. Chem. Lett.*, 2013, **4**, 1843–1849.
76 R. Nomura and N. Nakai, *Trans. Mater. Res. Soc. Jpn.*, 2003, **28**, 1287–1290.
77 F. Srouji, M. Afzaal, J. Waters and P. O'Brien, *Chem. Vap. Deposition*, 2005, **11**, 91–94.
78 G. Gurumoorthy, P. J. Rani, S. Thirumaran and S. Ciattini, *Inorg. Chim. Acta*, 2017, **455**, 132–139.
79 C. Gervas, M. D. Khan, S. Mlowe, C. Zhang, C. Zhao, R. K. Gupta, M. P. Akerman, P. Mashazi, T. Nyokong and N. Revaprasadu, *ChemElectroChem*, 2019, **6**, 2560–2569.
80 M. Congiu, L. G. S. Albano, F. Decker and C. F. O. Graeff, *Electrochim. Acta*, 2015, **151**, 517–524.
81 J. Yang, G. Zhu, Y. Liu, J. Xia, Z. Ji, X. Shen and S. Wu, *Adv. Funct. Mater.*, 2016, **26**, 4712–4721.
82 F. P. Andrew and P. A. Ajibade, *J. Coord. Chem.*, 2019, **72**, 1171–1186.
83 X. Zhang, Y. Liu, J. Gao, G. Han, M. Hu, X. Wu, H. Cao, X. Wang and B. Li, *J. Mater. Chem. A*, 2018, **6**, 7977–7987.
84 M. He, L. Zhu, Y. Liu, H. Wen, Y. Hu and B. Li, *Catal. Sci. Technol.*, 2020, **10**, 3622–3634.
85 B. B. Kaul and K. B. Pandeya, *Transition Met. Chem.*, 1979, **4**, 112–114.